Analysis of Tower Shadow Effects on Battery Lifetime in Standalone Hybrid Wind-Diesel-Battery Systems

Analysis of Tower Shadow Effects on Battery Lifetime in Standalone Hybrid Wind-Diesel-Battery Systems

***Abstract*— In a standalone hybrid wind-diesel-battery system, the battery lifetime is often optimistically over-predicted by hybrid system designers and battery manufacturers. As a result, battery replacement takes place more often than required. One of the reasons is due to the underestimation of battery wear from the short charge-discharge cycles, otherwise known as microcycles. A microcycle takes place when the power generation closely matches the load demand. The detrimental effect of microcycles on a battery-based standalone hybrid renewable energy system was previously investigated, however only from the perspective of short-term renewable energy fluctuations. This research paper provides new insight on battery lifetime reduction, resulting from microcycles which are generated through the tower shadow phenomena. Downwind wind turbines are considered here as their tower shadow effects are more significant compared to the upwind counterpart. This paper briefly presents the modeling of tower shadow profiles for both tubular and four-leg tower configurations. Experimental results have shown that the microcycles due to this non-ideal effect are significant in a battery-based standalone hybrid system. The quantification of the battery lifetime reduction due to this effect is demonstrated. Finally, the paper concludes with a sensitivity analysis of the battery lifetime reduction for different tower configurations, operating at different load conditions.**

***Index Terms*—tower shadow, hybrid wind-diesel-battery system, microcycles, battery lifetime, off-grid, isolated, renewable energy, experiment, modeling**

I. INTRODUCTION

THE concept of off-grid hybrid renewable energy systems (RESs) is known as an attractive and sustainable solution for supplying clean electricity to autonomous consumers. Typically, this applies to the communities that are located in remote or islanded areas where it is not cost-effective to extend the grid facilities to these regions. In addition, the use of diesel generators in these remote locations have been proven to be uneconomical due to the difficult terrain which translates into high fuel transportation costs [1] [2]. The use of hybrid systems that couple renewable energy sources with diesel generation reduces diesel fuel usage. However, to date, a common design standard for off-grid systems has yet to be found and the reliability of batteries within an off-grid hybrid system still needs to be assessed [3].

Because of the stochastic behavior of wind, relying solely on wind turbines is insufficient to meet the varying load demand [4]. Additionally, these fluctuations can potentially cause stability problem and degradation on power quality, especially in a weak grid system [5]. For larger wind turbines, wind power fluctuations can be somewhat mitigated through blade pitch control. However, this technology is uncommon in small wind turbines [6]. Batteries are recognized as a widely adopted energy storage solution to smooth wind power fluctuations, especially in rural areas of developing countries and in some cases, they are also considered as the main electricity carrier [7]. Within these regions, low-income households have been utilizing batteries to power lighter loads, such as radios and TVs for a few hours during the night [8].

In most applications, batteries are operating distinctly in either charging or discharging mode. Battery cycling is one of the major factors which contributes to degradation, typically characterized by its depth of discharge (DoD) [9]. Short-term charge-discharge cycling may occur in a RES where generators and loads are operating simultaneously [10]. Battery degradation can become more severe when the renewable sources vary significantly. For instance, a wind turbine with turbulent wind input can generate considerable power fluctuations into the system at frequencies up to several Hertz [10] [11]. However, since battery current is generally measured in terms of mean values over an interval of 1 minute or longer, the short charge-discharge cycles or microcycles are often overlooked by designers. This may lead to an over-optimistic view on the battery lifetime.

Microcycles are defined as a fast and continuous change of battery current with a change of direction, typically with a period in the range of seconds [12]. At any time interval, the battery current can be broken down into two components; the DC value and a spectrum of frequencies that cause no net flow of current when integrated over time [10]. The resulting microcycles from the power electronics converters can be easily removed using appropriate filtering circuits [11]. On the other hand, it has been found that lower frequency and high magnitude AC components can cause charge-discharge cycling of the active material, which may cause battery wear [10] [13].

Experiments in the past have indicated that the microcycles have a detrimental effect on the battery performance [12] [14] [15]. In this work, the focus is to investigate the effect that wind turbine tower shadow has on a battery storage system in an off-grid hybrid system. Hypothetically, the oscillations generated from the tower shadow effects are believed to have

negative consequences on the battery lifetime. As far as the author is aware, other studies on the tower shadow effects have not given attention to off-grid systems. In addition, many have considered tower shadow modeling of upwind, three-bladed wind turbines. The downwind tower shadow effect has been modeled, but yet to be investigated experimentally.

This paper is structured as follows. The modeling of downwind tower shadow is described in Section II, including both tubular and four-leg tower configurations. Section III briefly explains the off-grid hybrid system experimental setup which was used to investigate the battery lifetime degradation due to tower shadow effects. In Section IV, the propagation of tower shadow effects at different stages of the hybrid system is analyzed. A comparison of battery lifetime reduction due to tower shadow from both tubular and four-leg tower configurations is performed. In addition, a battery lifetime reduction sensitivity analysis was carried out with different load conditions. Finally, conclusions derived from the research are given in Section V.

II. Modeling of Tower Shadow Effect in Downwind Wind Turbines

In small wind turbine applications, tubular and four-leg (lattice) towers are commonly being used to support the nacelle and the wind turbine rotor. In this section, the modeling of these tower shadow profiles is briefly discussed. In particular, it is based on the Gaia Wind 11 kW downwind wind turbine [16]. It is important to note that the modeling presented in this work can be adapted for other types of wind turbine. The Gaia Wind wind turbine was chosen due to the information and hardware availability.

Reiso highlighted several steady wake models which can be used to describe the mean velocity deficit for downwind turbines; these are the Powles, Blevins, Schlichting, and jet wake models [17]. In 1983, Powles formulated a tower shadow model for downwind mounted rotors [18]. He identified that a cosine squared model predicts the tower shadow fairly accurately in the region of 3 - 6 tower diameters downstream [18]. Blevins' model has some similar features compared to Powles' model. However, it was originated from fluid dynamics to describe the wake behind a cylinder [19]. The Schlichtings' wake model originated from boundary layer theory with the idea of a frictional surface in the interior of the flow [20]. The jet wake model is adopted in this work as it was developed for time-series simulation [21]. It can be implemented in Matlab/Simulink and programmed using a dSPACE controller to emulate tower shadow effect in real-time.

A. Downwind Configuration – Tubular Tower

The jet wake model [21] was established to represent a quasi-steady reference for the time varying CFD wake velocity behind a cylindrical tower. This model is based on the boundary layer solution for a jet flowing into a fluid at rest [21]. The axial and lateral velocity components were developed as:

$$u(x,\eta) = \frac{\sqrt{3}}{2}\sqrt{\frac{K\sigma}{x}}(1 - tanh^2(\eta)) \tag{1}$$

$$v(x,\eta) = \frac{\sqrt{3}}{4}\sqrt{\frac{K\sigma}{x}}(2\eta(1 - tanh^2(\eta) - \tanh(\eta)) \tag{2}$$

where $\eta = \sigma\frac{y}{x}$, x and y are non-dimensional (with respect to tower radius) Cartesian co-ordinates in the tower cross section, as demonstrated in Fig. 1.

σ is an empirical constant equal to 7.67 [21]. K is the kinematic momentum defined as:

$$K = \frac{J_{\mathrm{m}}}{\rho} \tag{3}$$

where:

ρ: Air density (kg/m^3)

J_{m}: momentum deficit behind the tower

The derived J_{m} expression [21] in terms of tower parameters can be written as:

$$J_{\mathrm{m}} = \frac{U_0^2 D}{2}\frac{\rho}{\pi}\left[\frac{1}{8} + \frac{16}{3\pi}\right]C_{\mathrm{d}}^2 \tag{4}$$

where:

D: Tower diameter (m)

U_0^2: Free stream velocity (m/s)

C_{d}: Drag coefficient of the tower

In order to ease the implementation of time-series simulation, equation (1) can be converted from a function of y (lateral distance) to a function of r (radial distance) and θ (azimuthal angle) as follows:

$$u(x,r,\theta) = \frac{\sqrt{3}}{2}\sqrt{\frac{K\sigma}{x}}\left(1 - tanh^2\left(\sigma\frac{r\sin\theta}{x}\right)\right) \tag{5}$$

It should be noted that this equation only valid for $90° \leq \theta \leq 270°$. For simplicity purposes, the tower shadow effect is assumed to be absent above the horizontal level of the hub.

B. Downwind Configuration – Four-leg Tower

An alternative tower configuration for small wind turbines is the four leg tower (also known as a lattice tower), connected by diagonal beams. For simplification purposes, only the four main legs are considered in this work. In addition, each leg was assumed to be cylindrical in shape. The authors in [22] performed CFD simulations on the axial wind velocity for tubular and four-leg tower configurations, respectively. With these assumptions, the jet wake model described above was programmed in Matlab/Simulink and it was used to estimate the tower shadow profile of the four-leg tower. For illustration

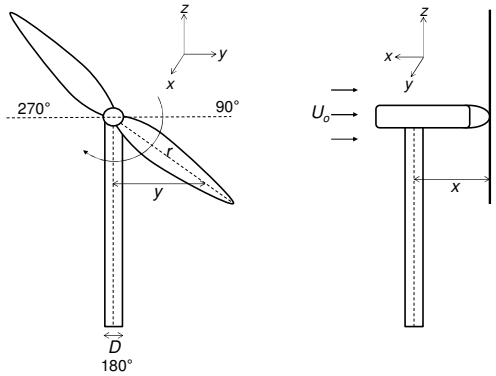

Fig. 1. Dimensions used in jet wake tower shadow formula

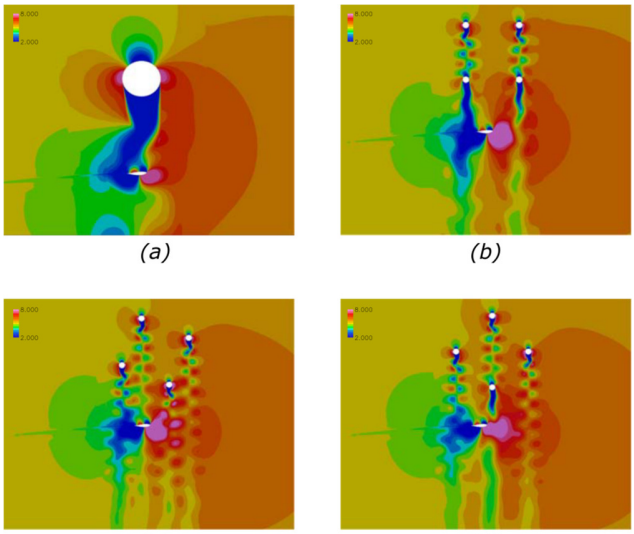

Fig. 2. CFD snapshot of axial wind velocity for a) tubular tower b) four-leg 0° orientation c) four-leg 22.5° orientation d) four-leg 45° orientation to the tower at 80% radius blade section [22]

purposes, Fig. 2 shows the extracted CFD snapshots [22] of the predicted wind flow patterns behind the towers.

As the Gaia wind turbine simply utilizes free-yaw mechanism, it is free to move around the tower based on the wind directions. Therefore, different tower shadow profiles can be generated due to the difference in yaw angles relative to the rotor plane. In this work, three orientations of the tower with respect to the rotor plane are considered. These are 0°, 22.5°and 45°, respectively. Fig. 3 shows the top view of the wind turbine with three different orientations. The estimated Gaia wind turbine lattice tower dimension is shown in Fig. 3 (a). The distance between each leg was approximated as 1.2 m. Each leg was represented as a cylindrical shape with a diameter of 0.2 m. For the sake of direct comparison with the tubular tower described above, the distance between the lattice tower center and the rotor plane was also set to 3 m.

Using the same principles from Fig. 3 (a), the dimensions for the case of 22.5° and 45° orientations can be easily derived from geometry. Then, the jet wake model was utilized to estimate the wind deficit caused by each leg, at 70% radius blade section. At this blade section, half of the rotor area was beyond the radius and the other half was within. Therefore, the velocity profile was represented. Using the Gaia wind turbine dimensions as tabulated in Table I [23], the simulated tower shadow profiles for the considered orientations are shown in Fig. 4. The analytically formulated tower shadow profiles capture the qualitative behavior of the simulated profiles in the

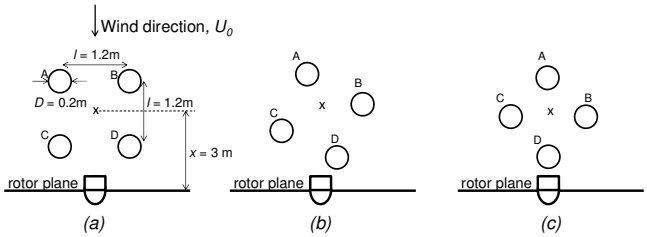

Fig. 3. Four-leg configuration with a) 0º orientation b) 22.5º orientation and c) 45 º orientation relative to the rotor plane, respectively

TABLE I
GAIA WIND TURBINE PARAMETERS FOR TOWER SHADOW COMPUTATIONS

Parameters	*Values*
Undisturbed wind speed, U_0	8 m/s
Blade radius, R	6.5 m
Hub height	18 m
Tower type	Tubular
Air density, ρ (kg/m^3)	1.225
Tower drag coefficient, C_d	0.4
Tower diameter, D	0.8 m
Distance from the blade to tower midline, x	3.0 m
Sigma, σ	7.67

literature [22]. The 0° lattice configuration produced a narrower width of wind deficits than the tubular configuration due to the smaller leg diameter. At 0° lattice orientation, the two front legs (A & B) were positioned in-line with the other two legs (C & D), respectively. The wind speed deficit from the front legs was further reduced by leg C & D. Therefore, an accumulation of wind speed deficit was experienced when the blade by-passed the tower. Two wind speed dips were experienced by the blade as it was rotating from position 90° to 270°. At 180°, the wind speed experienced by the blade recovered to the maximum value before moving towards to the next leg. Similar analysis can be applied to the 22.5° and 45° orientations.

It can be visualized that the lattice configuration generates a more sophisticated tower shadow profile at varying degrees of orientation, compared to its tubular counterpart. Therefore, it is the interest of this research to compare and contrast the effect of these tower shadow profiles on the battery lifetime.

III. HYBRID SYSTEM LABORATORY SETUP

The overall block diagram of the hybrid system is shown in Fig. 5 and their corresponding components are shown in Fig. 6. Three single-phase Sunny Island (SI) inverters were used to form an isolated three-phase grid with the energy being supplied by the Rolls batteries (total capacity of 106 Ah). In

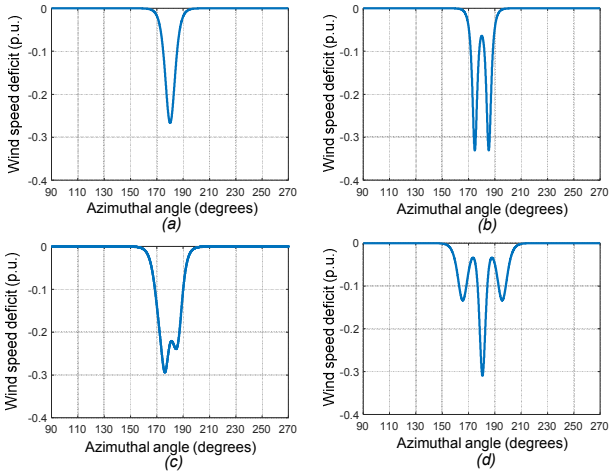

Fig. 4. Analytically derived downwind tower shadow profiles with l = 1.2 m for a) tubular tower b) four-leg 0° orientation c) four-leg 22.5° orientation d) four-leg 45° orientation to the tower

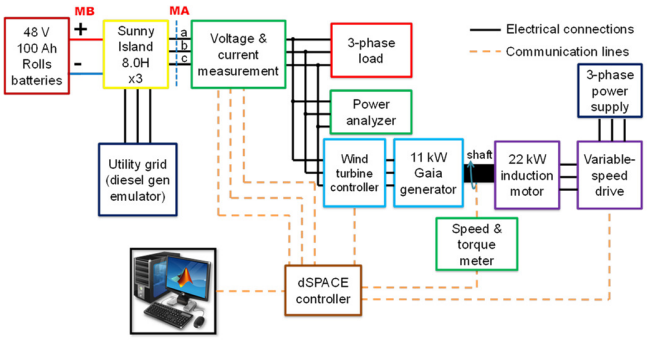

Fig. 5. Hybrid wind-diesel-battery laboratory setup

Fig. 6. Hybrid system lab setup equipment

reality, the Gaia 133-11 kW fixed speed wind turbine consists of 4 main components: the blades, the step-up gearbox, the induction generator and the wind turbine controller. The induction generator was connected to the isolated grid via a wind turbine controller. In this work, a 22 kW induction motor was used to emulate the wind energy, driving the induction generator. The motor was driven by a variable-speed AC drive (Parker SSD Drive). With the generator running at a near-constant speed, the torque can be controlled to emulate the varying mechanical torque input due to varying wind speeds. The torque input was fed through a dSPACE DS1103 controller. With the capability of programming different torque demand at the inverter drive, the tower shadow effect which causes a reduction in wind speed can be modeled. While the aerodynamics and inertia of the blade and gearbox were modeled in Simulink, the 11 kW generator's inertia effect on the induced microcycles was taken into consideration as the system was not scaled down.

A load bank was connected in parallel with the induction generator output. In the setup, the diesel generator was emulated using the utility grid. The diesel generator and the utility grid have the same terminal connections to the SI inverters and therefore, they are similar as seen from the inverters point of view. The diesel generator or the utility grid was used as a backup and they formed the three-phase grid automatically whenever the batteries state of charge (SOC) was low. The steady-state and dynamic analysis of the standalone hybrid system is presented in [24].

In another work, the characterization of the tower shadow effect using the wind turbine emulator was performed. The limitation of the induction machine drive system in responding to the tower shadow profiles has been identified through the frequency response test. In particular, the 10 Hz harmonic waveform which lies within the tower shadow profile can cause unwanted oscillations. It is not described in this paper due to space constraint. Therefore, the tower shadow profiles from a wind turbine can be emulated, while being aware that the limitations do exist when analyzing the results in the following sections.

IV. TOWER SHADOW EFFECT ON BATTERY LIFETIME

This section investigates the battery lifetime reduction as a result of tower shadow effect generated from the downwind wind turbine. The following subsections are dedicated to discussing the experimental measurement results of the emulated tower shadow using the described test rig and the process of estimating the batteries lifetime reduction as a consequence of these tower shadow effects. The power oscillations from the emulated tower shadow and their contribution to the charging and discharging microcycles are discussed. Battery degradation from both tubular and lattice towers are compared. Finally, a sensitivity analysis on battery lifetime was conducted with various load conditions.

A. Experimental Results of Tower Shadow Effect

Utilizing the analytically derived tubular and lattice tower shadow profiles from Fig. 4 as the wind inputs to the test rig, the pulsating power outputs with tower shadow effects were produced. Typically, the battery microcycles throughput would be the largest when the level of power generation within the system is approximately equal to the load. In this experiment, the wind speed of the system was set as 8 m/s, which corresponds to a power generation of about 8 kW. On the other hand, the resistive load demand was set to match this figure as close as possible so that the maximum number of microcycles can be computed with this scenario. Therefore, the load demand was set as 8 kW. Any small energy excess or deficit was balanced by the batteries. For base case reference purposes, the measurement results without including the tower shadow effect are given in Fig. 7. It can be observed that the measured power difference between the generator and the load (Fig. 7 (b)) was rather constant. Within the measurement

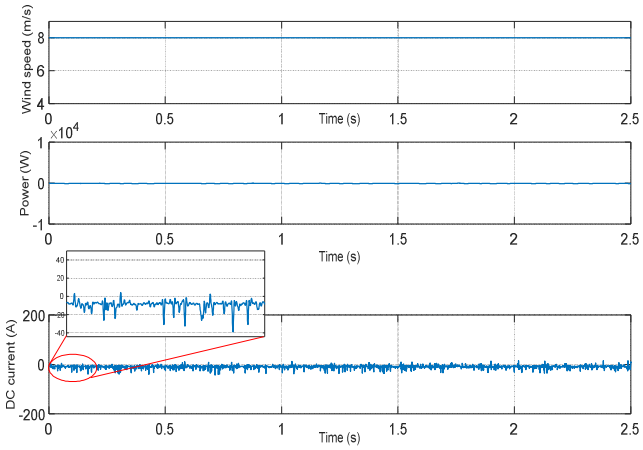

Fig. 7. Measurement results without tower shadow effect *(a)* fixed wind speed experienced by the blades *(b)* power difference between the generator and the load (point MA) *(c)* batteries DC current (point MB)

period, the battery DC current has negligible zero-crossings, which is indicated in Fig. 7 (c). Thus, the microcycle throughput was almost zero for this case. A closer inspection on the waveform revealed that the DC current was slightly shifted towards the negative values. This negative sign convention indicates that the batteries were constantly charging. This test also demonstrated that the computed number of microcycles in this work had excluded other possible contributions such as load or wind fluctuations.

Same measurements were performed for the case of the tubular tower, lattice tower with 0°, 22.5° and 45° degree orientations, as illustrated from Fig. 8 to Fig. 11, respectively. In all scenarios, the batteries were subjected to rapid charge and discharge which can be observed from the DC current plots. In addition, the oscillations after each tower shadow effect were noticed, except for the case of lattice tower with 45° degree orientation. This issue has been previously discussed and it can be attributed to the unstable operation of the generator, due to the presence of resonant frequency of approximately 10 Hz. The analytically derived tower shadow profile of the lattice tower with 45° degree orientation generates low amplitude of harmonics at around 10 Hz, thus the oscillation was not apparent in this particular scenario.

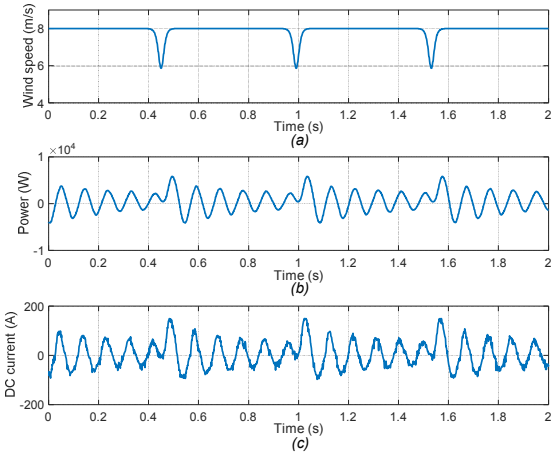

Fig. 8. Measurement results with tubular tower shadow effect *(a)* modeled wind speed experienced by the blades *(b)* power difference between the generator and the load (point MA) *(c)* batteries DC current (point MB)

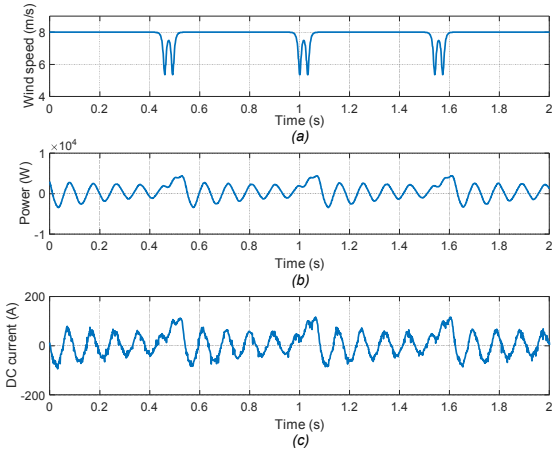

Fig. 9. Measurement results with lattice 0° orientation tower shadow effect *(a)* modeled wind speed experienced by the blades *(b)* power difference between the generator and the load (point MA) *(c)* batteries DC current (point MB)

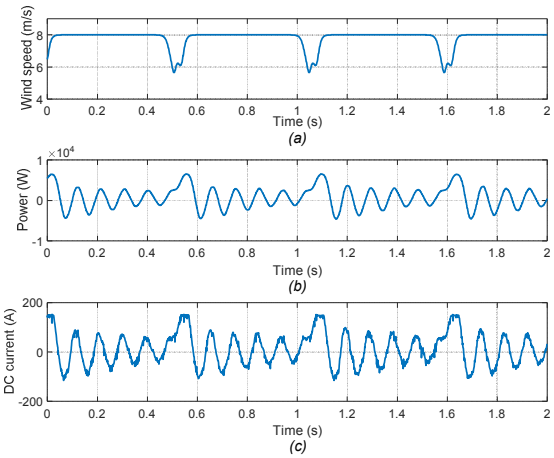

Fig. 10. Measurement results with lattice 22.5° orientation tower shadow effect *(a)* modeled wind speed experienced by the blades *(b)* power difference between the generator and the load (point MA) *(c)* batteries DC current (point MB)

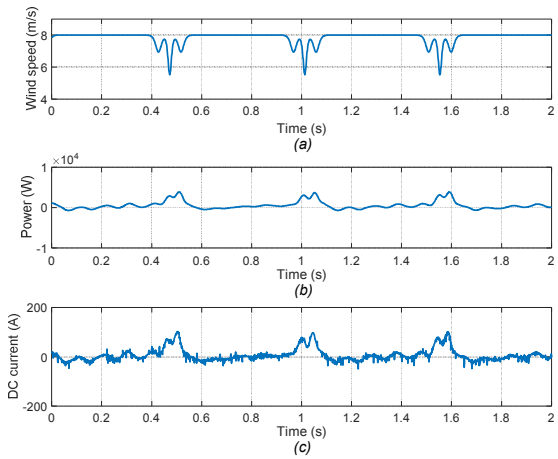

Fig. 11. Measurement results with lattice 45° orientation tower shadow effect *(a)* modeled wind speed experienced by the blades *(b)* power difference between the generator and the load (point MA) *(c)* batteries DC current (point MB)

In order to have a fair comparison while computing the battery lifetime reduction, the contribution of microcycles from the 10 Hz oscillation was discounted from the analysis. In this case, the microcycles contributed by the 10 Hz oscillation was characterized separately and it is shown in Fig. 12. With this approach, the battery lifetime caused by only the tower shadow effect was computed more accurately.

B. Battery Lifetime Modeling

Being able to predict the lifetime of a battery is of great importance in the initial stage of hybrid system design as it involves the decision of determining the operating conditions and replacement planning for batteries [25]. Manufacturers cannot test their batteries for a full range of applications due to the huge amount of time and costs involved, in addition to the lack of detailed knowledge concerning the use of batteries in various applications [25]. Various kinds of battery lifetime models are available. However, it is not practical to consider highly sophisticated battery lifetime model which include aging processes and various extreme non-linear stress factors. Fortunately, simplified battery life estimation has been developed, such as the rain-flow cycle counting model [26].

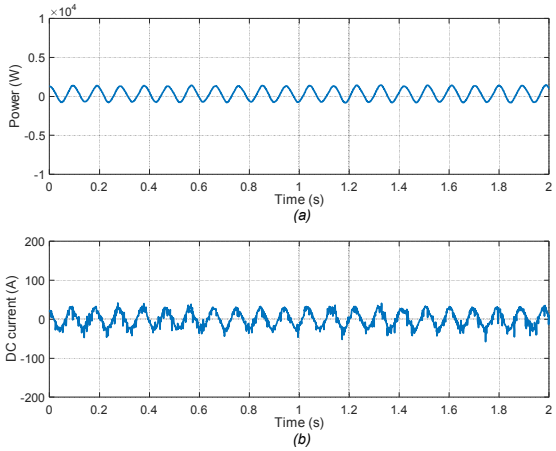

Fig. 12. Microcycles induced by 10 Hz harmonic which will be subtracted from the calculation of battery lifetime

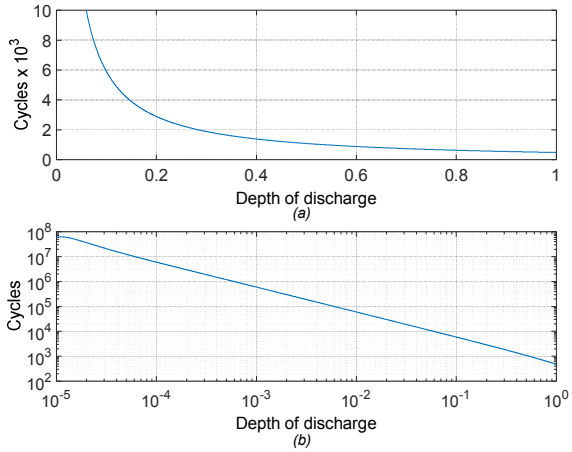

Fig. 13. (a) Cycles-to-failure versus depth of discharge for a typical deep-cycle lead-acid battery (b) Extrapolated cycles to failure versus depth of discharge for the same battery on a logarithmic scale [28]

This method assumes that the battery lifetime is primarily a function of DoD cycles [27]. Experimental validations have been conducted against several other battery life models and the results show that the cycle counting algorithm generates a relatively more accurate prediction [26]. In renewable energy applications, this method has been successfully employed in [28] and [29]. In addition, this algorithm is chosen to be implemented in a commercial hybrid system sizing software, known as the HYBRID2 [27]. This methodology requires the following assumptions to be made and they were considered primarily in fatigue analysis [25]:

- The stress events can be defined to induce only a small amount of incremental loss of lifetime. It can frequently occur until the battery fails.
- The loss of lifetime caused by a stress event is independent of previous stress events and the present battery state-of-health.
- The process of battery deterioration is either independent of the sequence of the stress events or the stress events which occur are distributed statistically throughout the lifetime of the battery. This also means that the battery is not assumed to be operated first at float operation for half of its lifetime and then subsequently cycled for the other half of its lifetime, but float operation and cycling happen more or less alternatively.

In this work, a cycles-to-failure versus DoD curve was employed and it is shown in Fig. 13 (a) [28]. The partial discharge cycles within the range less than 0.1 were extrapolated so that battery lifetime due to microcycles can be considered, as depicted in Fig. 13 (b). An adjusted cycle-to-failure curve was resulted, which effectively allows the microcycles to be evaluated. The corresponding relationship is approximated by a polynomial curve fit [28]:

$$C_{\mathrm{d}} = -1.345e^{-12}d^{-4} + 1.495e^{-7}d^{-3} - 0.001507d^{-2} + 601.5d^{-1} - 122.5 \quad (6)$$

where:

C_{d}: Cycles to failure at a depth of discharge d

d: Depth of discharge

If the number of cycles-to-failure for a given depth of discharge, d is C_{d}, then the fraction of battery life used in one full cycle of range, d can be written as $1/C_{\mathrm{d}}$. If i different cycle ranges are considered each with N_i cycles, the total battery life fraction consumed, W can be computed as a summation of each individual cycle as [28]:

$$W = \sum_{i=i_{min}}^{i=i_{max}} \frac{N_i}{C_{\mathrm{d}i}} \quad (7)$$

After certain cycles and when the accumulated fraction becomes 1.0, the battery is assumed to reach its end of life and it needs to be substituted with a new one.

In reality, it is challenging to measure the little changes in battery SOC caused by the occurrence of microcycles. Furthermore, an extended period of experimental running time, coupling with the highly sensitive transducers are required to produce an accurate measurement in the SOC changes. In order to facilitate this analysis, computer simulation is utilized as it is a cost-effective method to investigate the small changes in battery SOC. This can be achieved by using measured battery charge and discharge currents as an input to the simulation model, as shown in Fig. 14. The current controlled source emulates the measured current profile by acting as the current supply and demand from the lead-acid battery. Finally, the SOC profile can be analyzed from the battery model.

A more useful quantification on the battery lifetime is to consider a longer term operation of the system. However, as mentioned before, this is not a practical solution and therefore, several assumptions are made in this work. First, the overall objective was set upon finding the microcycle impacts on the

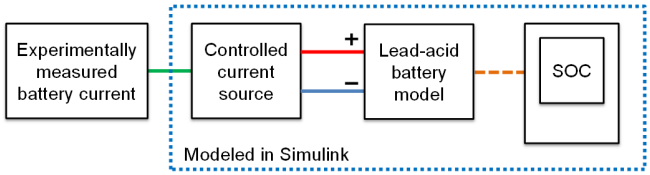

Fig. 14. Methodology to simulate batteries SOC using Simulink

battery lifetime for a period of 1 year. At the year-end of operation, the batteries lifetime reduction due to only the effect tower shadow is sought. In order to achieve this, the time-series yearly operational approach to calculate the battery throughput [10] is not applicable as it is challenging to negate other factors which contribute to battery degradation. In addition, high computational effort is required when the applied time-step is very small. In a real off-grid scenario, the wind turbines are commonly sized at higher power rating than the peak load demand. However, they are not always operating at their rated capacity and with the highly stochastic nature of the wind and load demand, the probability for the batteries to run at zero-crossings is high. For simplicity purposes, it is reasonable to assume that in one day, the microcycles induced from tower shadow effect occur for 30 minutes (less than 1% of one day). Nevertheless, it is greatly acknowledged that the occurrence of microcycles in reality can be influenced by other factors such as daily and seasonal variations of renewable energy sources, load demand and the operational strategy of the hybrid system.

The experimental measurement was conducted for a period of 10 s, although the results demonstrated from Fig. 8 to Fig. 12 only show 2 s of measurement results. Hence, the first step was to calculate the undergone microcycles by the battery within the period of 10 s. This was performed by the rain-flow cycle counting algorithm. The corresponding cycle-to-failure value was then computed using equation (6) and (7).

From the sizing study in [30], it was shown that the optimum storage size of a hybrid wind-diesel-battery system is 90 kWh. This corresponds to 1875 Ah for a 48 V system. Therefore, the battery capacity in the Simulink model was set to these figures in order to simulate a more practical situation. Fig. 15 to Fig. 18 demonstrate the simulated SOC profiles for tubular, lattice 0° orientation, lattice 22.5° orientation and lattice 45° orientation tower shadows, respectively. A comparison between these SOC profiles shows that the batteries undergone fewer polarity reversals when the lattice tower was positioned at 45° against the rotor plane.

Using the above-described modeling approach and the assumptions made, the battery lifetime reduction in a year due to tower shadow effects was computed. However, it was determined that the contribution of the 10 Hz oscillation in battery lifetime reduction worked out to be about 12%. This

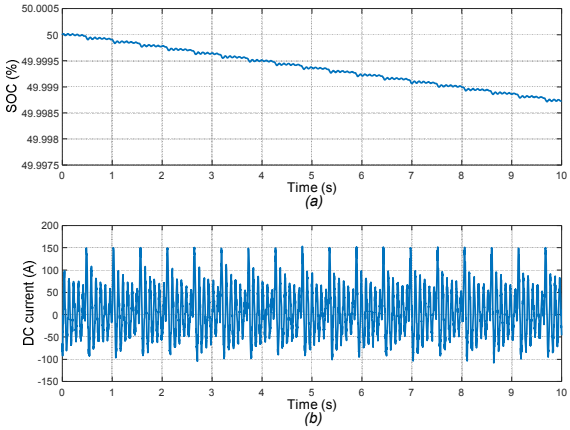

Fig. 15. Tubular tower simulated (a) battery SOC with measured (b) battery current

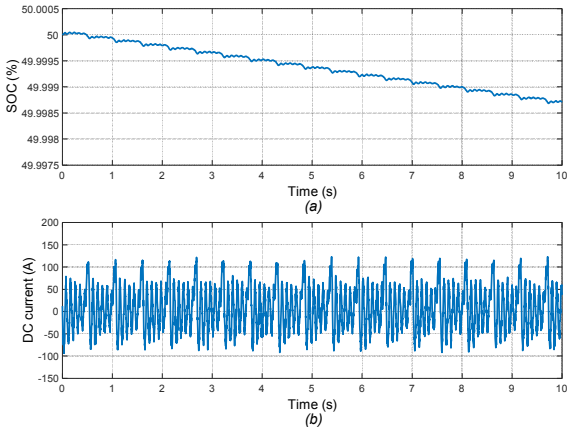

Fig. 16. Lattice 0° orientation tower simulated (a) battery SOC with measured (b) battery current

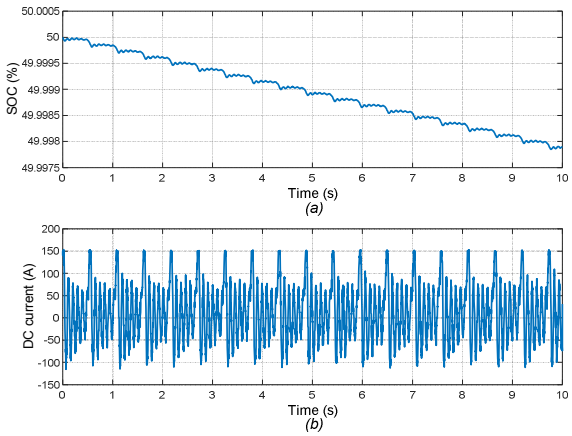

Fig. 17. Lattice 22.5° orientation tower simulated (a) battery SOC with measured (b) battery current

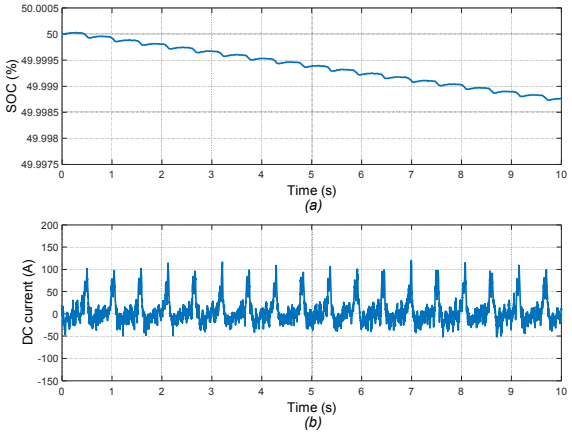

Fig. 18. Lattice 45° orientation tower simulated (a) battery SOC with measured (b) battery current

was discounted from the calculated battery lifetime reduction, in particular for the tubular, lattice 0° orientation and lattice 22.5° orientation tower configurations as they are subjected to the influence of 10 Hz oscillation. Note that this is case specific for the utilized test rig. Other test rigs might be influenced by other oscillation frequencies and this depends heavily on the drive system response.

Fig. 19 shows the comparison of the battery lifetime reduction for the tubular, lattice 0° orientation, lattice 22.5°

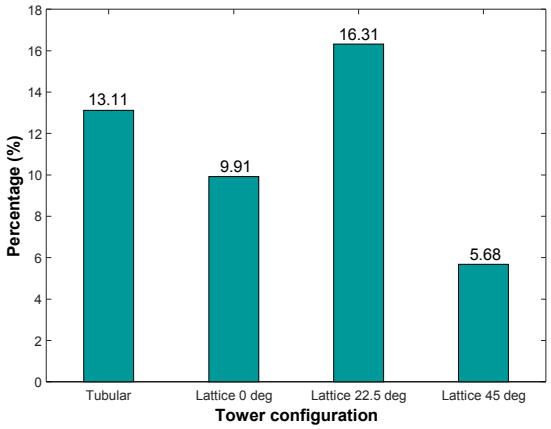

Fig. 19. Battery lifetime reduction in a year from microcycles for different tower configurations

and lattice 45° orientation tower configurations, respectively. The battery lifetime reductions in one year (in percentages) are solely attributed to the tower shadow effect. It can be observed that the lattice tower incurred a more complex effect on the battery lifetime results, which highly depends on its orientation. The 22.5° orientation has the most detrimental effect on the battery lifetime, recording 16.31% in a year, as opposed to 5.68% when the tower is positioned at 45° against the rotor plane. In reality, the wind turbine orientation varies significantly depending on the wind direction. Although there is a possibility that the lattice tower has a lower impact on the battery lifetime, it is not considerably lower than the tubular tower if no appropriate planning on the lattice tower's position is taken into consideration. In particular, the wind direction of the specific site has to be studied. It is believed that by placing the lattice tower in an optimum way with respect to the wind direction, there is a higher probability that minimal tower shadow effect may be imposed on the batteries. In this way, the benefits of using a lattice tower in an off-grid system can be maximized, in addition to its lower cost structure compared to the tubular counterpart. However, the lattice tower is potentially more dangerous for the birds as they might be exposed to the rotational motion of the blades due to the availability of resting steels for them to get near to. In addition, it is perceived to have a higher visual impact compared to the tubular towers. Therefore, many considerations need to be assessed before making the choice of tower structure.

C. Sensitivity Analysis on Tower Shadow Effects on Battery Lifetime

As mentioned before, the battery microcycles throughput is the largest when the power generation closely matches the load [10]. However, previous studies focused on the occurrence of microcycles as a result of variability of renewable resources and load fluctuations. In this section, the objective is to investigate if this concept holds true when the microcycles are contributed from the tower shadow effect. The assumption used in this work was that the microcycles due to tower shadow effect on average occur 30 minutes every day. Finally, the battery lifetime reduced in a year was determined.

In order to study the microcycles effect at different load conditions, a sensitivity analysis was carried out. Different offset current values were artificially added to the measured current profiles to emulate different load conditions. This approach simplifies the analysis and same current profile with different offset values were compared among each other. An example of demonstrating the addition of an offset current to the tubular tower's generated current profile is shown in Fig. 20. In this case, a fixed value of -40 A was added to the current profile. This translates to a reduction in load demand of about 2 kW.

In this work, it is proposed that the current values of 10 A, 20 A, 30 A, -10 A, -20 A, -30 A, -40 A and -50 were added to current profiles of all the tower configurations. Again, the 10 Hz oscillation current profile was discounted while calculating the microcycles contribution from the tubular, lattice 0° orientation and lattice 22.5° orientation. Fig. 21 shows the battery lifetime reduced percentages as a result of microcycles with different load conditions. It can be observed that the battery lifetime reduction trend varies in a non-linear fashion despite the linear change in current magnitude. Interestingly, the battery lifetime for tubular, lattice 0° orientation and lattice 45° orientation were most severely affected when the current profiles were reduced by 10 A (load reduction of 500 W). For lattice 22.5° orientation, the highest reduction in battery lifetime occurred when the current was reduced by 20 A (which correspond to a load reduction of 1 kW). These results

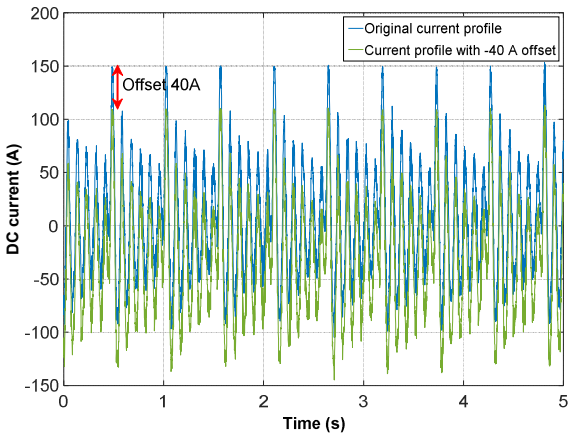

Fig. 20. An example to demonstrate an offset current being added to the original current profile

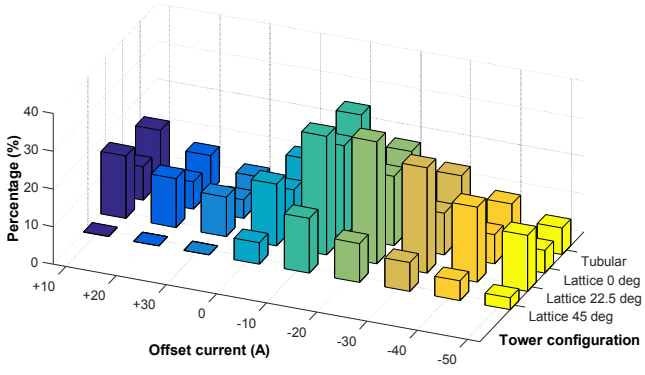

Fig. 21. Battery lifetime reduction in a year from microcycles for different tower configurations and load conditions

are in contrast to the previous fact which claimed that the highest battery throughput due to microcycles should occur when the load matches the generation [10]. This may be explained by the difference in tower shadow profiles generated from different tower configurations. As expected, the battery throughput due to the microcycles reduces as the difference between power generation and the load becomes larger. Using the assumptions mentioned, the reduction in battery lifetime lies within the range of about 5% to 27% in one year, depending on the tower's configuration.

It is believed that the magnitude of the tower shadow effects can be mitigated mechanically or electronically. In terms of mechanical approach, the tower can be redesigned with a different architecture. Electronically, a power electronics module coupled with the appropriate filters can theoretically attenuate the magnitude of the power dip as a result of tower shadow. One potential solution to absorb the power fluctuations is through the utilization of hybrid energy storage systems (ESS). In the scale of laboratory and in terms of practicality purposes, a hybrid battery-supercapacitor energy storage system is a promising solution to begin. The aim of such solution is to introduce the supercapacitor to absorb high-frequency power surges while reducing the required battery power rating, degree of discharge and power losses of the overall system. The supercapacitor technology has the advantage of a long cycle life, high cycle efficiency, short response time, and high power capacity which can be used to compensate the limitations of the conventional battery system [31]. The hybrid approach takes advantage of the two complementing technologies to provide significant power and energy capacities. Some simulation and experimental work have been dedicated to the development of power electronics interfaces and energy managements for the hybrid battery-supercapacitor ESS technology [32] [33] [34]. The battery lifetime gained from the additional components involved would require an economic analysis to be carried out. In addition, the methodology of sizing of the supercapacitors can be developed to achieve the optimum financial and technical performances.

The study in this work has opened up several research questions:

- What is the optimum tower structure design for a small wind turbine in an off-grid system which minimizes the effect of tower shadow on the battery systems?
- In what way a controller can help to minimize the effect of tower shadow?
- Can power electronics technologies solve the problem of tower shadow and is it worth implementing it in a hybrid system?

V. CONCLUSION

In conclusion, this paper described and discussed the modeling approach and the experimental work which focused on the battery lifetime reduction due to the tower shadow effect in an off-grid hybrid wind-diesel-battery system. The non-ideal behavior, such as the oscillation of the test rig was considered and the approach to "compensate" this through post-processing are demonstrated. The characteristics of the tower shadow profiles from both tubular and lattice towers perspective are clearly demonstrated. In particular, their individual effect on the battery lifetime is studied. It was found out that the microcycles indeed reduce the battery lifetime in a quantifiable manner. The finding here is important for system designers whilst sizing the hybrid system during planning stages as it is very often the battery lifetime is assumed to last optimistically longer than in reality.

REFERENCES

[1] M. S. Ismail, M. Moghavvemi, and T. M. I. Mahlia, "Techno-economic analysis of an optimized photovoltaic and diesel generator hybrid power system for remote houses in a tropical climate," *Energy Conversion and Management,* vol. 69, pp. 163-173, 2013.

[2] M. Bortolini, M. Gamberi, A. Graziani, and F. Pilati, "Economic and environmental bi-objective design of an off-grid photovoltaic–battery–diesel generator hybrid energy system," *Energy Conversion and Management,* vol. 106, pp. 1024-1038, 2015.

[3] M. E. Menconi, S. dell'Anna, A. Scarlato, and D. Grohmann, "Energy sovereignty in Italian inner areas: Off-grid renewable solutions for isolated systems and rural buildings," *Renewable Energy,* vol. 93, pp. 14-26, 2016.

[4] J. K. Kaldellis, *Stand-Alone and Hybrid Wind Energy Systems: Technology, Energy Storage and Applications*: Woodhead Publishing Ltd, 2010.

[5] D. Weisser and R. S. Garcia, "Instantaneous wind energy penetration in isolated electricity grids: concepts and review," *Renewable Energy,* vol. 30, pp. 1299-1308, 2005.

[6] L. Wang, X. Tang, and X. Liu, "Blade Design Optimisation for Fixed-Pitch Fixed-Speed Wind Turbines," *ISRN Renewable Energy,* vol. 2012, p. 8, 2012.

[7] P. Maher, N. P. A. Smith, and A. A. Williams, "Assessment of pico hydro as an option for off-grid electrification in Kenya," *Renewable Energy,* vol. 28, pp. 1357-1369, 2003.

[8] A. A. Lahimer, M. A. Alghoul, F. Yousif, T. M. Razykov, N. Amin, and K. Sopian, "Research and development aspects on decentralized electrification options for rural household," *Renewable and Sustainable Energy Reviews,* vol. 24, pp. 314-324, 2013.

[9] C. Zhou, K. Qian, M. Allan, and W. Zhou, "Modeling of the Cost of EV Battery Wear Due to V2G Application in Power Systems," *IEEE Transactions on Energy Conversion,* vol. 26, pp. 1041-1050, 2011.

[10] A. J. Ruddell, A. G. Dutton, H. Wenzl, C. Ropeter, D. U. Sauer, J. Merten, C. Orfanogiannis, J. W. Twidell, and P. Vezin, "Analysis of battery current microcycles in autonomous renewable energy systems," *Journal of Power Sources,* vol. 112, pp. 531-546, 2002.

[11] A. Tani, M. B. Camara, and B. Dakyo, "Energy Management in the Decentralized Generation Systems Based on Renewable Energy-Ultracapacitors and Battery to Compensate the Wind/Load Power Fluctuations," *IEEE Transactions on Industry Applications,* vol. 51, pp. 1817-1827, 2015.

[12] C. Ropeter, H. Wenzl, H. P. Beck, E. A. Wehrmann, J. W. Twidell, and D. U. Sauer, "The impact of microcycles on batteries in different applications," in *Proceedings of the 18th Electric Vehicle Symposium (EVS18), Berlin*, 20 October 2001.

[13] C. J. Zhan, X. G. Wu, S. Kromlidis, V. K. Ramachandaramurthy, M. Barnes, N. Jenkins, and A. J. Ruddell, "Two electrical models of the lead-acid battery used in a dynamic voltage restorer," *IEE Proceedings - Generation, Transmission and Distribution,* vol. 150, pp. 175-182, 2003.

[14] G. Lutzemberger, "Cycle life evaluation of lithium cells subjected to micro-cycles," in *5th International Youth Conference on Energy (IYCE)*, 2015, pp. 1-5.

[15] M. Ceraolo, A. D. Donato, C. Miulli, and G. Pede, "Microcycle-based efficiency of hybrid vehicle batteries," in *IEEE Conference Vehicle Power and Propulsion*, 2005, pp. 233-237.

[16] "User Manual - Gaia-Wind 11 kW Turbine," *Gaia-Wind Ltd.*, United Kingdom, August 2008.

[17] M. Reiso, "The Tower Shadow Effect in Downwind Wind Turbines," PhD Thesis, Department of Civil and Transport Engineering, Norwegian University of Science and Technology (NTNU), Norway, May 2013.

[18] S. R. J. Powles, "The effects of tower shadow on the dynamics of a horizontal axis wind turbine," *Wind Engineering,* vol. 7, pp. 26-42, 1983.

[19] R. D. Blevins, *Flow-Induced Vibrations*. New York: Van Nostrand Reinhold, 1990.

[20] H. Schlichting and K. Gersten, *Boundary-Layer Theory*. Berlin: Springer, 2000.

[21] H. A. Madsen, J. Johansen, N. N. Sørensen, G. C. Larsen, and M. H. Hansen, "Simulation of low frequency noise from a downwind wind turbine rotor," in *45th AIAA Aerospace Sciences Meeting and Exhibit*, pp. 1-12, 2007.

[22] F. Zahle, H. A. Madsen, and N. N. Sørensen, "Research in Aeroelasticity EFP-2007-II," *Danmarks Tekniske Universitet, Risø Nationallaboratoriet for Bæredygtig Energi.*

[23] M. Molinari, M. Pozzi, D. Zonta, and L. Battisti, "In-field testing of a steel wind turbine tower," in *International Modal Analysis Conference (IMAC) XXVIII*, Florida USA, 2010.

[24] L. K. Gan, J. K. H. Shek, and M. A. Mueller, "Modelling and experimentation of grid-forming inverters for standalone hybrid wind-battery systems," in *International Conference on Renewable Energy Research and Applications (ICRERA)*, 2015, pp. 449-454.

[25] H. Wenzl, I. Baring-Gould, R. Kaiser, B. Y. Liaw, P. Lundsager, J. Manwell, A. Ruddell, and V. Svoboda, "Life prediction of batteries for selecting the technically most suitable and cost effective battery," *Journal of Power Sources,* vol. 144, pp. 373-384, 2005.

[26] H. Bindner, T. Cronin, P. Lundsager, J. F. Manwell, U. Abdulwahid, and I. Baring-Gould, "Lifetime modelling of lead acid batteries," Risø National Laboratory, Roskilde, Denmark, April 2005.

[27] J. F. Manwell, A. Rogers, G. Hayman, C. T. Avelar, and J. G. McGowan, "Hybrid2- A hybrid system simulation model -Theory Manual," Renewable Energy Research Laboratory, Department of Mechanical Engineering, University of Massachusetts, November 1998.

[28] A. M. Gee, F. V. P. Robinson, and R. W. Dunn, "Analysis of Battery Lifetime Extension in a Small-Scale Wind-Energy System Using Supercapacitors," *IEEE Transactions on Energy Conversion,* vol. 28, pp. 24-33, 2013.

[29] J. Li, A. M. Gee, M. Zhang, and W. Yuan, "Analysis of battery lifetime extension in a SMES-battery hybrid energy storage system using a novel battery lifetime model," *Energy,* vol. 86, pp. 175-185, 2015.

[30] L. K. Gan, J. K. H. Shek, and M. A. Mueller, "Hybrid wind–photovoltaic–diesel–battery system sizing tool development using empirical approach, life-cycle cost and performance analysis: A case study in Scotland," *Energy Conversion and Management,* vol. 106, pp. 479-494, 2015.

[31] Y. Kim, J. Koh, Q. Xie, Y. Wang, N. Chang, and M. Pedram, "A scalable and flexible hybrid energy storage system design and implementation," *Journal of Power Sources,* vol. 255, pp. 410-422, 2014.

[32] L. Wei and G. Joos, "A power electronic interface for a battery supercapacitor hybrid energy storage system for wind applications," in *IEEE Power Electronics Specialists Conference (PECS)*, 2008, pp. 1762-1768.

[33] L. Wei, G. Joos, and J. Belanger, "Real-Time Simulation of a Wind Turbine Generator Coupled With a Battery Supercapacitor Energy Storage System," *IEEE Transactions on Industrial Electronics,* vol. 57, pp. 1137-1145, 2010.

[34] Z. Haihua, T. Bhattacharya, T. Duong, T. S. T. Siew, and A. M. Khambadkone, "Composite Energy Storage System Involving Battery and Ultracapacitor With Dynamic Energy Management in Microgrid Applications," *IEEE Transactions on Power Electronics,* vol. 26, pp. 923-930, 2011.